ISSN 2304-3415, Russian Open Medical Journal
2026. Volume 15. Issue 3 (September). Article CID e0309
DOI: 10.15275/rusomj.2026.0309

Original article

Boosting Antitumor Activity: CuO Nanoparticles Enhance Pemetrexed Efficacy and Increase *hsa-miR-548c-3p* Expression in Human Lung Cancer

Sepideh Mokabberi [1], Nahid Babaei [1], Hadi Esmaeili Gouvarchin Ghaleh [2], Gholamreza Farnoosh [3]

[1] Department of Molecular Cell Biology and Genetics, Bu.C., Islamic Azad University, Bushehr, Iran
[2] Applied Virology Research Center, Biomedicine Technologies Institute, Baqiyatallah University of Medical Sciences, Tehran, Iran
[3] Applied Biotechnology Research Centre, New Health Technologies Institute, Baqiyatallah University of Medical Sciences, Tehran, Iran

Received 26 August 2025, Revised 6 February 2026, Accepted 9 April 2026

© 2025, Russian Open Medical Journal

Abstract: *Background and objective* — Lung cancer, particularly non-small cell lung cancer (NSCLC), is a leading cause of cancer-related death. Pemetrexed (PEM) is recognized as an effective chemotherapy drug. However, its efficacy is often compromised by resistance and side effects. Copper oxide nanoparticles (CuO NPs) are promising agents due to their unique characteristics, which can improve drug delivery and cytotoxicity. The objective of this study was to evaluate the simultaneous effect of CuO NPs on enhancing the antitumor activity of PEM in human lung cancer cells and to investigate changes in *hsa-miR-548c-3p* expression in lung cancer cells.
Methods — After culturing A549 cancer cells, various concentrations of PEM and CuO NPs were applied to determine the IC_{50} value. The cells were then exposed to half the IC_{50} concentration of PEM, both with and without CuO NPs, for 48 h. The assessment included measurements of cell viability, apoptosis, lactate dehydrogenase (LDH) release, reactive oxygen species (ROS), and the relative expression levels of *hsa-miR-548c-3p*, *TYMS*, *CASP8*, and *CASP9*.
Results — The study showed that concomitant use of PEM with CuO NPs nanoparticles resulted in decreased cell viability (P<0.05) and increased apoptosis, ROS production, and LDH release compared with the control group and the group receiving the either drug alone (P<0.05). Concomitant use also increased the expression of *hsa-miR-548c-3p*, *CASP8*, and *CASP9* (P<0.05), while decreasing *TYMS* expression compared with the control group (P<0.05).
Conclusion — Based on the results of this study, it can be concluded that the combination of CuO NPs with PEM may enhance the efficacy of the latter chemotherapeutic drug.

Keywords: lung cancer, pemetrexed, CuO nanoparticles, *hsa-miR-548c-3p*, apoptotic pathway, cytotoxicity.

Cite as Mokabberi S, Babaei N, Esmaeili Gouvarchin Ghaleh H, Farnoosh G. Boosting antitumor activity: CuO nanoparticles enhance pemetrexed efficacy and increase *hsa-miR-548c-3p* expression in human lung cancer. *Russ Open Med J* 2026; 15: e0309.

Correspondence to Hadi Esmaeili Gouvarchin Ghaleh. Email: h.smaili69@yahoo.com.

Introduction

Lung cancer is one of the most common and deadly cancers worldwide. It is classified into two main types: non-small cell lung cancer (NSCLC) and small cell lung cancer (SCLC). NSCLC accounts for more than 80-85% of cases, while SCLC accounts for approximately 15-20% [1, 2]. Many patients are diagnosed with lung cancer at an advanced stage, which complicates treatment.

Available treatment methods include surgery, chemotherapy, radiation therapy, and targeted therapy [3]. Pemetrexed (PEM) is a chemotherapy drug developed for the treatment of NSCLC and certain other cancers. It acts as an antimetabolite, inhibiting cancer cell proliferation by blocking enzymes critical for DNA and RNA production, particularly dihydrofolate reductase (DHFR) and thymidylate synthase (*TYMS*) [4]. These enzymes play an important role in folate metabolism and nucleotide synthesis. By inhibiting them, PEM limits the resources required by cancer cells for growth and division, thereby promoting tumor shrinkage and disease control [4, 5]. Limitations of chemotherapy drugs include damage to healthy cells and serious side effects, low tumor permeability, and cancer cell resistance to drugs [6].

Nanoparticles (NPs) have significant potential to enhance the efficacy of chemotherapeutic agents by improving drug permeability and targeted delivery, and can also reduce side effects and facilitate targeted cancer treatment by increasing the formation of reactive oxygen species (ROS) and stimulating tumor cell apoptosis [7]. Copper oxide (CuO) NPs exhibit anticancer properties due to their antioxidant capabilities and ROS formation. As a result, cancer cell growth becomes inhibited. CuO NPs induce oxidative stress, leading to cell death, and can also function as targeted drug carriers, enhancing the efficacy of chemotherapy and reducing side effects [8]. Furthermore, studies show that CuO NPs show higher cytotoxicity towards human cells than to other metal oxide NPs. The anticancer effects of CuO NPs have been investigated in various types of cancer, including liver, lung, breast, cervical, and pancreatic cancer [9].

MicroRNAs (*miRNAs*) are non-coding RNAs that regulate gene expression by binding to messenger RNAs (mRNAs), influencing biological processes such as cell division, death, and migration

© 2026, LLC Science and Innovations, Saratov, Russia

[10]. Studies show that abnormal *miRNA* expression significantly contributes to the development and progression of various metabolic diseases. In cancer, altered *miRNA* levels can influence the expression of genes associated with cancer cell growth, with some functioning as oncogenes and others as tumor suppressors [11]. The *miR-548* gene family, comprising 69 poorly conserved primate-specific genes on human chromosomes, is critical for a variety of diseases. It generates mature *miR-548c-3p*, which has been identified as a regulatory factor in many cancers, including prostate, esophageal, thyroid, osteosarcoma, glioma, gallbladder, gastric, and breast cancers [12]. Furthermore, mounting evidence suggests that *miR-548* inhibits cancer cell proliferation and promotes apoptosis, acting as a tumor suppressor in the lung [13]. The present study aimed to investigate the antitumor effects of CuO NPs co-administered with PEM and to examine changes in *hsa-miR-548c-3p* expression in lung cancer cells.

Material and Methods

Experimental design

A549 cells (ATCC® CCL185™) were obtained from the Pasteur Institute of Iran and cultured in DMEM (Sigma, St. Louis, MO, USA) with 10% FBS at 37 °C in a 5% CO_2 atmosphere. Cells were exposed to different concentrations of PEM (1–12 µM) [14] and CuO NPs (Nanosany-Iran) (0, 2.5, 5, 10, 20, 40, 80, 100, 200, and 400 µg/mL) [15] for 24 and 48 h to determine the IC_{50} concentration. Afterwards, the cells were divided into four groups: control, CuO NPs-treated group, PEM-treated group, and combination therapy group receiving both CuO NPs and PEM. For treatment in the combination therapy group (CuO NPs + PEM), half the IC_{50} concentration was used.

Cell viability

After 48 h of treatment of A549 cells with CuO NPs, PEM, and a combination of CuO NPs and PEM, the culture medium was carefully removed from each well. Fresh culture medium (90 µL) was added to each well along with 10 µL of a 5 mg/mL MTT solution (resulting in a final concentration of 0.5 mg/mL). The plates were incubated for 4 h, and formazan crystal formation was observed under an inverted microscope. The medium was carefully removed, and 100 µL of DMSO (Sigma Aldrich, USA) was added to each well. After incubation for 30 minutes in order to dissolve the crystals, the resulting purple color was measured with an ELISA reader at a wavelength of 570 nm. All concentrations were tested in triplicate to ensure precision [14].

Apoptosis assay

We used fluorescent dyes, specifically acridine orange and ethidium bromide, to stain cell nuclei. Acridine orange can penetrate the membranes of living cells, while ethidium bromide only penetrates the membranes of dead cells. In this assay, living cells exhibit green fluorescence, while apoptotic cells change color from orange to red. A suspension of 10^4 cells in DMEM was placed in 24-well plates (500 µL per well) and incubated for 24 h. Then the wells were processed according to the experimental design. After 48 h, the treatment solutions were removed, and a mixture (250 µL) containing acridine orange and ethidium bromide (5 µg/mL of the former and 5 µg/mL of the latter in phosphate-buffered saline) were added for 2 min. Cells were subsequently examined by fluorescence microscopy [14].

LDH release assay

Lactate dehydrogenase (LDH) is an enzyme that serves as a marker of cell damage, and cytotoxicity assays rely on its release. This enzyme is present in eukaryotic cells and is released from the plasma membrane upon cell damage or death. We assessed LDH levels using the Kiazist kit (KLDH96): 10,000 cells were seeded into each well of a 96-well plate and incubated for 48 h. After that, treatment groups were applied, and 20 µL of Permi solution was added to each well. The plate was then incubated at room temperature for 1 h. To measure LDH, 50 µL from each well was transferred to a new plate, after which working buffer was added (50 µL). After 30 minutes of incubation at 37 °C in the dark, absorbance was measured at 570 nm [14].

Table 1. Hsa-miR-548c-3p and U48 sequences, and primers used for real-time qRT-PCR

miRNA	*Sequence*	*Primer sequence*
hsa-miR-548c-3p (MIMAT0003285)	CAAAAAUCUCAAUUACUUUUGC	Stem-loop primer: GTCGTATCCAGTGCAGGGTCCGAGGTATTCGCACTGGATACGACGCAAAAG Forward primer: GCACAGCCAAAAATCTCAATTAC Reverse primer: GTCGTATCCAGTGCAGGGT
U48 (NR_002745.1)	AGTGATGATGACCCCAGGTAACTCTTGAGTGT GTCGCTGATGCCATCACCGCAGCGCTCTGACC	Stem-loop primer: GTCGTATCCAGTGCAGGGTCCGAGGTATTCGCACTGGATACGACGGTCAG Forward primer: CTCTGAGTGTGTCGCTGATGCC Reverse primer: CCAGTGCAGGGTCCGAGGTA

qRT-PCR, real-time quantitative reverse transcription polymerase chain reaction.

Table 2. Primer sequences, annealing temperatures, and PCR product sizes shown in the (5'→3') direction

Gene		*Primer sequence (5'→3')*	*Length (bp)*	*Annealing temperature (°C)*	*Product size (bp)*
TYMS(NM_001071.4)	F	CTGGGGCAGATCCAACACAT	20	60	152
	R	ACACCCTTCCAGAACACACG	20		
CASP8(NM_001228.5)	F	CGGGGATACTGTCTGATCAT	20	57	127
	R	CAAAGGTCGTGGTCAAAGC	19		
CASP9(NM_001229.5)	F	TGGCTCCTGGTACGTTGA	18	57	99
	R	GAAACAGCATTAGCGACCC	19		
GAPDH(NM_002046.7)	F	TGACTTCAACAGCGACACCCA	21	61	121
	R	CACCCTGTTGCTGTAGCCAAA	21		

PCR, polymerase chain reaction; bp, base pairs.

© 2026, LLC Science and Innovations, Saratov, Russia

Table 3. Percentage viability and IC_{50} calculation for A549 cells after 24 and 48 h of treatment with PEM and CuO NPs

Group	*IC_{50} 24 hours*	*IC_{50} 48 hours*
PEM	4.766 µM	2.891 µM
CuO NPs	160.2 µg/ml	72.12 µg/ml

IC_{50}, half-maximal inhibitory concentration; PEM, pemetrexed; CuO NPs, copper oxide nanoparticles.

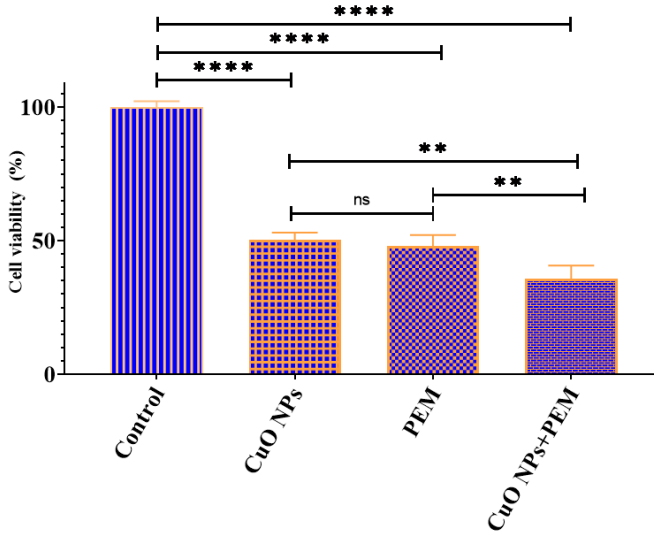

Figure 1. Post-treatment comparison of A549 cell viability with the study groups.

, *P*<0.01; **, *P*<0.0001; ns, *P*>0.05.

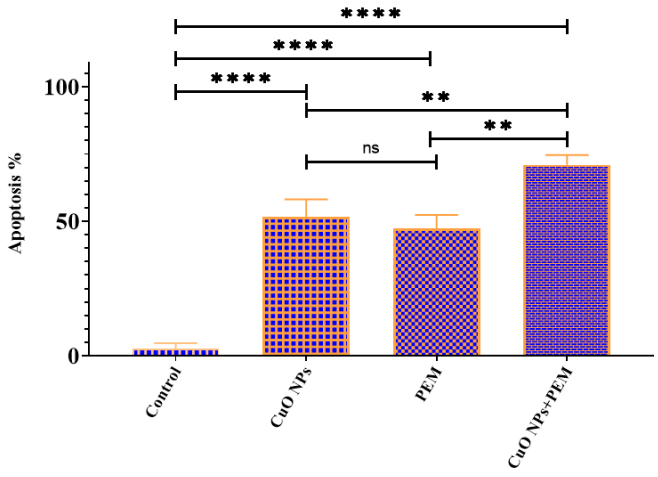

Figure 2. Post-treatment comparison of apoptosis in A549 cells with the study groups.

, *P*<0.01; **, *P*<0.0001; ns, *P*>0.05.

ROS production assay

ROS are reactive oxygen-containing molecules that are produced naturally in mitochondria or by external agents in cells. These radicals can damage cellular macromolecules, causing various tissue and cellular disorders, including cancer. Common types of ROS include superoxide radicals, hydroxyl radicals, and peroxides. In this assay, the 2',7'-dichlorofluorescein diacetate (DCFDA) dye was employed to measure ROS levels. This dye can penetrate living cells and be de-esterified by intracellular enzymes, after which it fluoresces upon reduction by specific ROS. Cells were seeded in a 96-well plate, treated accordingly, and then washed with ROS buffer. Afterwards, 100 µL of DCFDA working solution was added to each well and incubated in the dark at 37 °C for 45 min. Fluorescence intensity was then measured at wavelengths of 485/528 nm [14].

RNA extraction

RNA extraction from cell cultures was performed using the RNX Plus kit. First, 1 mL of the RNX Plus solution was mixed with 10^6 cells and transferred to a microtube. Next, 250 µL of cold chloroform was added, the mixture was vortexed, and then centrifuged for 15 min at 13,000 rpm at 4 °C. The resulting clear supernatant was carefully transferred to a new microtube, and 500 µL of isopropanol was added. This mixture was then centrifuged for another 15 min at 13,000 rpm at 4 °C, resulting in the formation of a white precipitate indicating the presence of RNA. Following this, 1 mL of 75% ethanol was added, and the sample was centrifuged for 10 min at 8,500 rpm at 4 °C. The supernatant was drained, and after the precipitate had dried, 50 µL of RNase-free water treated with diethyl pyrocarbonate (DEPC) was added. The quality and quantity of the isolated RNA were assessed using a NanoDrop spectrophotometer, after which the RNA was stored at -70 °C [14].

cDNA synthesis

The AddScript cDNA Synthesis Kit was used for cDNA synthesis. In this process, 1 µg of DNase I-treated RNA was placed in a 0.2 mL microtube. To it were added 1 µL of reverse transcriptase enzyme, 2 µL of dNTPs, 4 µL of buffer, and 3 µL of a mixture of oligo(dT) and random hexamer primers. The total volume was adjusted to 20 µL with DEPC-treated water. The mixture was then incubated for 60 min at 50 °C, followed by a 10-min incubation at 80 °C. The synthesized cDNA was stored at -21 °C until real-time PCR was performed. For miR cDNA synthesis, a specific primer was used instead of oligo(dT) and random hexamer primers, as detailed in *Table* 1 [14].

Real-time PCR

To assess changes in gene expression, we performed the SYBR Green-based real-time PCR according to the guidelines provided with the Parstus kit. First, 10 µL of the SYBR Green master mix was placed in a real-time PCR microtube. Then, 1 µL of a mixture containing the forward and reverse primers for the target gene, each at a concentration of 10 µM (as indicated in *Tables* 1 and 2), was added. Next, 1 µL of the prepared cDNA was added, and the final volume was adjusted to 20 µL with distilled water [14].

Statistical analysis

Statistical analysis and plotting of cell data were performed using GraphPad Prism, version 8.2.1. One-way analysis of variance (ANOVA) was employed to compare different groups. For all statistical evaluations, *P*<0.05 was considered statistically significant, and data are presented as mean ± standard error of the mean (SEM). Relative gene expression levels were estimated using the Relative Expression Software Tool (REST), version 2.0.13. Results obtained using REST were analyzed alongside cell data to ensure a thorough and comprehensive analysis.

© 2026, LLC Science and Innovations, Saratov, Russia

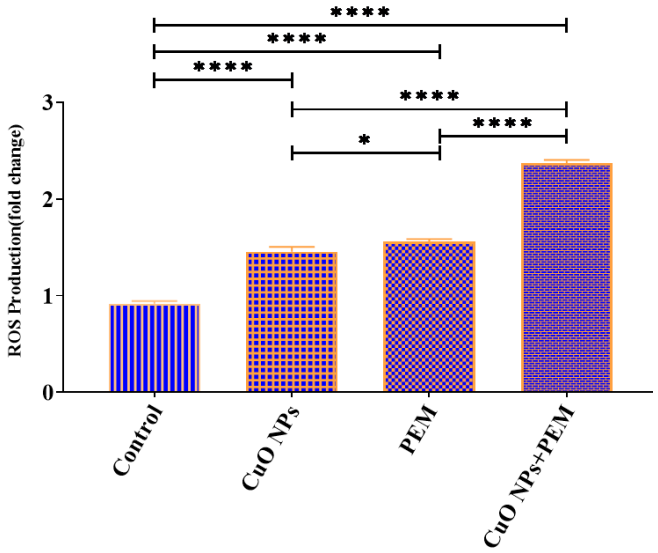

Figure 3. Post-treatment comparison of ROS formation in A549 cells with the study groups.

*, *P*<0.05; **, *P*<0.01; ****, *P*<0.0001; ns, *P*>0.05.

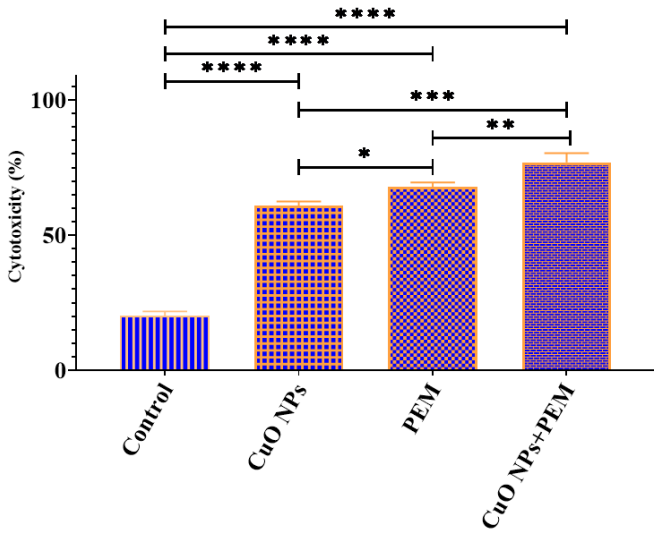

Figure 4. Post-treatment comparison of LDH release by A549 cells with the study groups.

*, *P*<0.05; **, *P*<0.01; ***, *P*<0.001; ****, *P*<0.0001; ns, *P*>0.05.

Results

IC_{50} for PEM and CuO NPs

IC_{50} concentrations for PEM and CuO NPs were determined using the MTT assay. IC_{50} measures the potency of a substance in terms of inhibiting a specific biological function: it indicates the amount required to achieve 50% inhibition of a biological process or component in vitro. *Table* 3 shows that the concentrations of PEM and CuO NPs required to achieve 50% inhibition of A549 cell growth after 24 h were 4.766 µM and 160.2 µg/mL, respectively, and after 48 h, 2.891 µM and 72.12 µg/mL.

Cell viability

The greatest reduction in cancer cell viability was observed after combination therapy with PEM and CuO NPs. *Figure* 1 shows that all treatments (CuO NPs, PEM, and their combination) statistically significantly reduced cell viability vs. the control group (*P*<0.05). Notably, the group receiving combination therapy (CuO NPs + PEM) experienced the most pronounced reduction in viability (*P*<0.05).

Apoptosis

The percentage of apoptosis in cancer cells after combination therapy with PEM and CuO NPs showed the most significant increase. *Figure* 2 illustrates the levels of apoptosis in the different treatment groups. The control group (no treatment) had the lowest levels of apoptosis, as no external factors were applied. In contrast, both PEM and CuO NPs significantly increased apoptosis, demonstrating a significant difference from the control group (*P*<0.0001). The combination therapy group (CuO NPs + PEM) exhibited the highest percentage of apoptosis (*P*<0.0001).

ROS

As shown in *Figure* 3, ROS formation significantly increased in all treatment groups vs. the control group (*P*<0.05). Furthermore, a significant increase in ROS production was observed in the combination therapy group (CuO NPs + PEM) vs. either monotherapy group (*P*<0.0001).

LDH

Figure 4 shows that LDH release levels increased significantly in all treatment groups vs. the control group (*P*<0.05). Furthermore, the combination therapy group (CuO NPs + PEM) demonstrated a highly significant increase in LDH release vs. either monotherapy group (*P*<0.0001).

Real-time PCR

The relative expression levels of *hsa-miR-548c-3p*, *CASP8*, and *CASP9* in cancer cells increased after all treatments compared with untreated cells, with a more significant increase in the combination therapy group than in the other groups (*P*<0.0001). In contrast, the relative expression of *TYMS* in cancer cells decreased after all treatments, and this reduction was more pronounced in the combination therapy group than in the other groups (*Figure* 5).

Discussion

Our study examined the combined effect of CuO NPs on enhancing the cytotoxic efficacy of PEM in human lung cancer cells, specifically the A549 cell line. The results showed that the use of PEM in conjunction with CuO NPs significantly reduced cell viability, increased the percentage of apoptosis, enhanced ROS production, and resulted in higher LDH release compared with the control group and groups treated with either agent alone.

Enhanced apoptosis in cancer cells is considered a beneficial indicator for cancer therapy, as apoptosis is a natural and regulated mechanism that promotes the removal of damaged and abnormal cells. This process plays a crucial role in maintaining cellular homeostasis and preventing the proliferation of potentially harmful cells [16]. Moreover, ROS formation is recognized as a critical mechanism in the induction of apoptosis. ROS can trigger

© 2026, LLC Science and Innovations, Saratov, Russia

various signaling pathways that lead to programmed cell death, thereby promoting the elimination of cancer cells and increasing the effectiveness of anticancer treatment [17]. When cancer cell membranes are damaged in cell culture, LDH is released into the culture medium. This process is recognized as a marker of cell damage and is widely used in toxicology studies and to assess the therapeutic effect on cancer cells. LDH release following membrane damage indicates cell death or severe cell damage [18].

Our findings confirmed that CuO NPs may act as a potentiating agent in PEM therapy, promoting apoptotic responses in cancer cells. Furthermore, the results showed that combination therapy resulted in increased expression of *hsa-miR-548c-3p*, as well as increased expression of *CASP8* and *CASP9*, while simultaneously diminishing *TYMS* expression. *MiR-548c-3p* reduces lung cancer cell proliferation by interfering with the galectin-3-mediated TLR4 signaling pathway. Furthermore, it increases the sensitivity of colorectal cancer cells to 5-fluorouracil by downregulating *TYMS* and *ABCG2* [13, 19].

High *TYMS* expression in malignant tumors is associated with reduced sensitivity to antifolate drugs, including PEM. In particular, *TYMS* are recognized as important enzymes involved in folate metabolism and nucleotide synthesis. A decrease in their activity may lead to inhibition of cancer cell growth and proliferation [20]. Takezawa et al. (2011) showed that NSCLC cells overexpressing *TYMS* exhibited significantly reduced sensitivity to the antiproliferative effect of PEM, compared with control cells. *TYMS* overexpression reduced the inhibition of DNA synthesis and the induction of apoptosis by PEM. Furthermore, tumors from *TYMS*-overexpressing cells in nude mice were resistant to PEM, indicating a negative correlation between *TYMS* levels and treatment response [20].

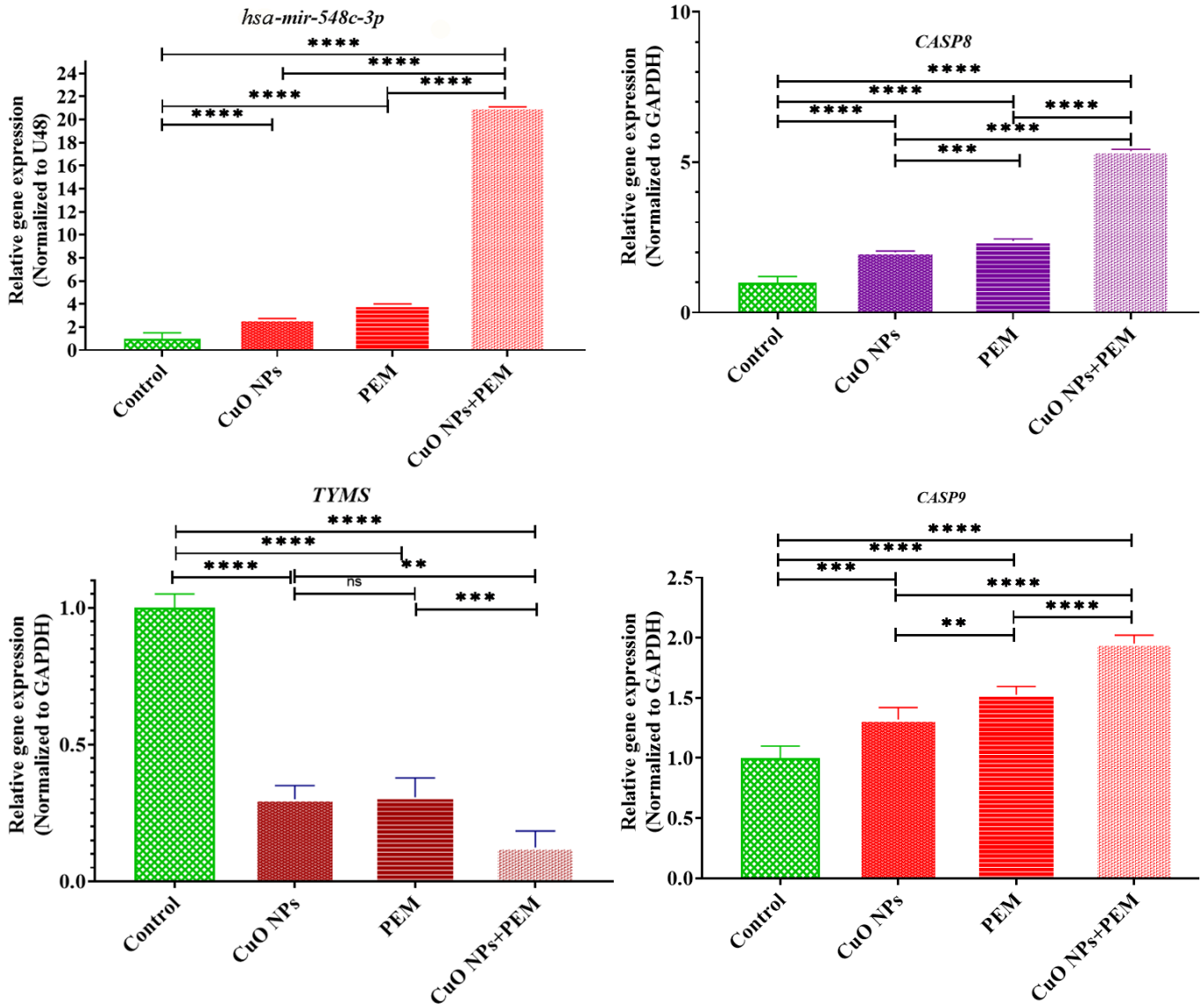

Figure 5. Relative expression of *hsa-miR-548c-3p*, *CASP8*, *CASP9*, and *TYMS*. Relative expression of *hsa-miR-548c-3p* in treated cells compared with untreated cells, normalized to RNU48. Relative expression of *TYMS*, *CASP8*, and *CASP9* in treated cells vs. untreated cells, normalized to GAPDH.

*, $P<0.05$; ns, $P>0.05$.

© 2026, LLC Science and Innovations, Saratov, Russia

Shafagh et al. (2015) found that CuO NPs selectively target cancer cells without affecting normal cells, as demonstrated by the MTT assay. Their cytotoxic effect on K562 cells was associated with ROS production, apoptosis induction confirmed by staining, and increased P53 expression, indicating a mitochondria-mediated apoptotic pathway [21]. Caspases play a crucial role in apoptosis. Caspase-8 is involved in the extrinsic pathway, while caspase-9 initiates the intrinsic apoptotic pathway [22]. The results of our study showed that CuO NPs and PEM induce apoptosis in lung cancer cells through both intracellular and extracellular pathways. Esmaeili Gouvarchin Ghaleh et al. (2019) reported a significant decrease in cell viability and an increase in apoptosis in MCF7 cells when treated with CuO NPs in combination with radiotherapy and hyperthermia vs. the control group. This treatment also resulted in increased ROS formation, LDH levels, and a significant increase in caspase-3 and caspase-9 activity, while caspase-8 activity remained unchanged [23].

Ghorbani Alvanegh et al. (2024) found that PEM treatment significantly increased LDH release after 24 h in Calu-6 cells. Treated samples showed increased levels *of hsa-miR-320a-3p* and *BAX*, while *VDAC1*, *STAT3*, *DHFR*, and *BCL2* expression decreased compared to control samples [24]. Furthermore, the researchers demonstrated that PEM reduced cell viability and increased apoptosis. After 48 hours, ROS production was higher than in control cells, and LDH release increased. Moreover, PEM significantly increased the expression of *hsa-miR-320a*, showing an approximately 12-fold increase [14].

Khalili et al. (2023) found that *miR-548c-3p* sensitized colorectal cancer cells to the chemotherapeutic drug 5FU by inhibiting the expression of *TYMS* and *ABCG2* genes [19]. Shi et al. (2015) showed that *miR-548-3p* was downregulated in breast cancer, and its overexpression inhibited cell proliferation while promoting apoptosis. *ECHS1* expression was increased in breast cancer tissues and was identified as a target of *miR-548-3p*. These results suggest the potential of *miR-548-3p* as a therapeutic target by regulating *ECHS1* expression [25]. Yao et al. (2020) reported that both *miR-423* and *miR-548c-3p* exhibited reduced expression in osteosarcoma. Increased levels of *miR-432* and *miR-548c-3p* in osteosarcoma cells were found to inhibit tumor cell proliferation and enhance apoptosis. These miRNAs may function as tumor suppressors in osteosarcoma, and their expression levels may serve as important indicators for assessing the benign or malignant nature of the disease [26].

Conclusion

This study revealed that the combination of PEM with CuO NPs significantly affects cellular responses, resulting in decreased survival and increased apoptosis in treated cells. Increased ROS production and LDH release indicate a cytotoxic effect of this combination therapy. Furthermore, increased levels of pro-apoptotic markers such as *hsa-miR-548c-3p*, *CASP8*, and *CASP9*, along with decreased levels of metabolic enzymes such as *TYMS*, suggest a shift in cellular pathways that may enhance the efficacy of PEM. These results highlighted the potential of this combination strategy to improve cancer treatment outcomes, which warrants further examination of its mechanisms and clinical application. Limitations of the study include the lack of in vivo validation, which may impact the generalizability of the results. Furthermore, focusing solely on specific biomarkers limits understanding of broader molecular mechanisms. The potential long-term effects and safety of CuO NPs have not been thoroughly investigated.

Acknowledgements

This study is part of Ms. Sepideh Mokabberi's PhD thesis. The authors express their gratitude to everyone who assisted us in this research.

Author contributions

SM, NB, HEGG, and GF developed the theoretical formalism, performed the analytical calculations, and conducted the numerical modeling. The authors contributed to the final version of the manuscript. NB supervised the project. Zigap AI was used to check this article for plagiarism.

Funding

The authors declare that no external funds, grants, or other support were received during the preparation of this manuscript.

Data availability

The datasets generated and/or analyzed during this study are available from the corresponding author upon reasonable request.

Ethical approval and consent to participate

The Ethics Committee of Baqiyatallah University of Medical Sciences approved the protocols of this study (IR.BPUMS.REC.1402.306).

Conflict of interest

The authors declare no conflicts of interest.

References

1. Padinharayil H, Varghese J, John MC, Rajanikant GK, Wilson CM, Al-Yozbaki M, et al. Non-small cell lung carcinoma (NSCLC): Implications on molecular pathology and advances in early diagnostics and therapeutics. *Genes Dis* 2023; 10(3): 960-989. https://https://doi.org/10.1016/j.gendis.2022.07.023.
2. Hendriks LEL, Remon J, Faivre-Finn C, Garassino MC, Heymach JV, Kerr KM, et al. Non-small-cell lung cancer. *Nat Rev Dis Primers* 2024; 10(1): 71. https://doi.org/10.1038/s41572-024-00551-9.
3. Tang FH, Wong HYT, Tsang PSW, Yau M, Tam SY, Law L, et al. Recent advancements in lung cancer research: A narrative review. *Transl Lung Cancer Res* 2025; 14(3): 975-990. https://doi.org/10.21037/tlcr-24-979.
4. Komiya T, Memmott RM, Blumenthal GM, Bernstein W, Ballas MS, De Chowdhury R, et al. A phase I/II study of pemetrexed with sirolimus in advanced, previously treated non-small cell lung cancer. *Transl Lung Cancer Res* 2019; 8(3): 247-257. https://doi.org/10.21037/tlcr.2019.04.19.
5. Li T, Huang JB, Lu JG, Li R, Wang Y, Shi XR, et al. Plasma thymidylate synthase and dihydrofolate reductase mRNA levels as potential predictive biomarkers of pemetrexed sensitivity in patients with advanced non-small cell lung cancer. *J Thorac Dis* 2020; 12(12): 7313-7319. https://doi.org/10.21037/jtd-20-3185.
6. Davodabadi F, Sajjadi SF, Sarhadi M, Mirghasemi S, Hezaveh MN, Khosravi S, et al. Cancer chemotherapy resistance: Mechanisms and recent breakthrough in targeted drug delivery. *Eur J Pharmacol* 2023; 958: 176013. https://doi.org/10.1016/j.ejphar.2023.176013.
7. Sabir S, Thani ASB, Abbas Q. Nanotechnology in cancer treatment: revolutionizing strategies against drug resistance. *Front Bioeng Biotechnol* 2025; 13: 1548588. https://doi.org/10.3389/fbioe.2025.1548588.
8. Abdolmaleki S, Aliabadi A, Khaksar S. Unveiling the promising anticancer effect of copper-based compounds: a comprehensive

© 2026, LLC Science and Innovations, Saratov, Russia

review. *J Cancer Res Clin Oncol* 2024; 150(4): 213. https://doi.org/10.1007/s00432-024-05641-5.

9. Abdollahzadeh H, Pazhang Y, Zamani A, Sharafi Y. Green synthesis of copper oxide nanoparticles using walnut shell and their size dependent anticancer effects on breast and colorectal cancer cell lines. *Sci Rep* 2024; 14(1): 20323. https://doi.org/10.1038/s41598-024-71234-4.
10. Nunes S, Bastos R, Marinho AI, Vieira R, Benício I, de Noronha MA, et al. Recent advances in the development and clinical application of miRNAs in infectious diseases. *Noncoding RNA Res* 2024; 10: 41-54. https://doi.org/10.1016/j.ncrna.2024.09.005.
11. Singh V, Sen A, Saini S, Dwivedi S, Agrawal R, Bansal A, et al. MicroRNA significance in cancer: An updated review on diagnostic, prognostic, and therapeutic perspectives. *EJIFCC* 2024; 35(4): 265-284. https://pubmed.ncbi.nlm.nih.gov/39810890.
12. Tan PY, Wen LJ, Li HN, Chai SW. MiR-548c-3p inhibits the proliferation, migration and invasion of human breast cancer cell by targeting E2F3. *Cytotechnology* 2020; 72(5): 751-761. https://doi.org/10.1007/s10616-020-00418-3.
13. Chen X, Chen Y, Hu Q, Chen X, Huang L. MiR-548c inhibits lung cancer cell proliferation through suppression of Galectin-3-mediated TLR4 signaling pathway. *Int J Clin Exp Med* 2018; 11(2): 581-592. https://e-century.us/files/ijcem/11/2/ijcem0055106.pdf.
14. Ghorbani Alvanegh A, Esmaeili Gouvarchin Ghaleh H, Mohammad Ganji S. The Growth of A549 cell line is inhibited by pemetrexed through up-regulation of hsa-MiR-320a expression. *Adv Biomed Res* 2024; 13: 50. https://doi.org/10.4103/abr.abr_483_23.
15. Bhavana S, Kusuma CG, Gubbiveeranna V, Sumachirayu CK, Ravikumar H, Nagaraju S. Green route synthesis of copper oxide nanoparticles using Vitex altissima [L] leaves extract and their potential anticancer activity against A549 cell lines and its apoptosis induction. *Inorganic and Nano-Metal Chemistry* 2024; 54(10): 1012-1025. https://doi.org/10.1080/24701556.2022.2081195.
16. Mirzayans R. What is apoptosis and why is it inhibited by the most important tumor suppressor (p53)? *Int J Mol Sci* 2025; 26(21): 10505. https://doi.org/10.3390/ijms262110505.
17. An X, Yu W, Liu J, Tang D, Yang L, Chen X. Oxidative cell death in cancer: Mechanisms and therapeutic opportunities. *Cell Death Dis* 2024; 15(8): 556. https://doi.org/10.1038/s41419-024-06939-5.
18. Kari S, Subramanian K, Altomonte IA, Murugesan A, Yli-Harja O, Kandhavelu M. Programmed cell death detection methods: A systematic review and a categorical comparison. *Apoptosis* 2022; 27(7-8): 482-508. https://doi.org/10.1007/s10495-022-01735-y.
19. Khalili E, Afgar A, Rajabpour A, Aghaee-Bakhtiari SH, Jamialahmadi K, Teimoori-Toolabi L. MiR-548c-3p through suppressing *Tyms* and *Abcg2* increases the sensitivity of colorectal cancer cells to 5-fluorouracil. *Heliyon* 2023; 9(11): e21775. https://doi.org/10.1016/j.heliyon.2023.e21775.
20. Takezawa K, Okamoto I, Okamoto W, Takeda M, Sakai K, Tsukioka S, et al. Thymidylate synthase as a determinant of pemetrexed sensitivity in non-small cell lung cancer. *Br J Cancer* 2011; 104(10): 1594-1601. https://doi.org/10.1038/bjc.2011.129.
21. Shafagh M, Rahmani F, Delirezh N. CuO nanoparticles induce cytotoxicity and apoptosis in human K562 cancer cell line via mitochondrial pathway, through reactive oxygen species and P53. *Iran J Basic Med Sci* 2015; 18(10): 993-1000. https://pubmed.ncbi.nlm.nih.gov/26730334.
22. Aral K, Aral CA, Kapila Y. The role of caspase-8, caspase-9, and apoptosis inducing factor in periodontal disease. *J Periodontol* 2019; 90(3): 288-294. https://doi.org/10.1002/JPER.17-0716.
23. Esmaeili Govarchin Ghaleh H, Zarei L, Mansori Motlagh B, Jabbari N. Using CuO nanoparticles and hyperthermia in radiotherapy of MCF-7 cell line: synergistic effect in cancer therapy. *Artif Cells Nanomed Biotechnol* 2019; 47(1): 1396-1403. https://doi.org/10.1080/21691401.2019.1600529.
24. Ghorbani Alvanegh A, Arpanaei A, Esmaeili Gouvarchin Ghaleh H, Mohammad Ganji S. MiR-320a upregulation contributes to the effectiveness of pemetrexed by inhibiting the growth and invasion of human lung cancer cell line (Calu-6). *Mol Biol Rep* 2024; 51(1): 310. https://doi.org/10.1007/s11033-024-09207-z.
25. Shi Y, Qiu M, Wu Y, Hai L. MiR-548c-3p functions as an anti-oncogenic regulator in breast cancer. *Biomed Pharmacother* 2015; 75: 111-116. https://doi.org/10.1016/j.biopha.2015.07.027.
26. Yao J, Tan W, Wu W, Ye R, Li Y, Chen Y. Effects of miR-432 and miR-548c-3p on the proliferation and invasion of osteosarcoma cells. *J BUON* 2020; 25(3): 1562-1568. https://pubmed.ncbi.nlm.nih.gov/32862605.

Authors:
Sepideh Mokabberi – PhD Student, Department of Molecular Cell Biology and Genetics, Islamic Azad University, Bushehr, Iran. https://orcid.org/0009-0003-6068-9110.
Nahid Babaei – PhD, Assistant professor, Department of Molecular Cell Biology and Genetics, Islamic Azad University, Bushehr, Iran. https://orcid.org/0000-0002-6968-1268.
Hadi Esmaeili Gouvarchin Ghaleh – PhD, Associate Professor, Applied Virology Research Center, Biomedicine Technologies Institute, Baqiyatallah University of Medical sciences, Tehran, Iran. https://orcid.org/0000-0001-8562-2295.
Gholamreza Farnoosh – PhD, Associate Professor, Applied Biotechnology Research Centre, New Health Technologies Institute, Baqiyatallah University of Medical Sciences, Tehran, Iran. https://orcid.org/0000-0001-8951-892X.

© 2026, LLC Science and Innovations, Saratov, Russia